Single-mode coupling efficiencies of type-II spontaneous parametric down-conversion: Collinear, noncollinear, and beamlike phase matching

Osung Kwon, Young-Wook Cho, and Yoon-Ho Kim*
Department of Physics, Pohang University of Science and Technology (POSTECH), Pohang, 790-784, Korea
(Received 25 September 2008; published 21 November 2008)

We report a series of experimental studies on single-mode fiber coupling of entangled photon pairs in type-II spontaneous parametric down-conversion. We experimentally compare the single-mode coupling efficiencies for three different phase matching regimes of bulk type-II spontaneous parametric down-conversion: collinear, noncollinear, and beamlike. Our experiment shows that the beamlike scheme provides the best single-mode coupling efficiency.

Entanglement is one of the most essential resources for quantum information. In photonic quantum information research, entangled photon states are most often generated via the process of spontaneous parametric down-conversion (SPDC), in which a higher energy pump photon is split into a pair of lower energy photons in a noncentrosymmetric crystal [1]. The photons involved in the SPDC process must satisfy the phase matching condition, the energy conservation and the momentum conservation, which is often categorized into two: type I and type II. In type-I SPDC, the down-converted photon pairs have the same polarization [2,3] and in type-II SPDC, they are orthogonally polarized [4].

Other significant differences between the type-I and type-II SPDC are spectral and spatial emission properties of the photons. For example, type-II SPDC has significantly narrower single and joint spectra than those of type-I SPDC [5,6]. Furthermore, unlike type-I SPDC which has a rather simple ring-type transverse emission pattern due to the degenerate nature of the polarization state of the photon pair, type-II SPDC emission forms two rings, one belonging to the extraordinary ray and the other to the ordinary ray of the crystal. Thus, type-II SPDC is known to be able to exhibit three distinctive transverse emission patterns: collinear [7,8], noncollinear [4], and beamlike [5,9,10].

Recently, there has been great interest in optimally coupling entangled photons of SPDC into single-mode optical fibers for quantum information applications. Experimentally, huge improvement of the entangled-photon flux in a single-mode optical fiber has been achieved using a relative simple spatial mode mapping method [11–16]. Theoretically, recent studies on type-I and type-II SPDC single-mode coupling attempt to provide the coupling efficiency upper bounds for a number of experimental conditions [17–19]. These analytical predictions, however, have not been subject to extensive experimental tests so far mainly because experiments to date have been mostly focused on maximizing the collection efficiency for noncollinear type-II SPDC to achieve a high-efficiency fiber-coupled source of polarization entangled photon pairs [11–14].

In this paper, we report a set of experimental studies on single-mode coupling of entangled photon pairs of type-II SPDC. In particular, we explicitly compare the biphoton single-mode coupling efficiencies of the entangled photon pairs in type-II SPDC for the three phase matching conditions: collinear, noncollinear, and beamlike. It is found that, as theoretically discussed in Ref. [19], the collinear case indeed exhibits better biphoton single-mode coupling efficiency than that of the noncollinear case. Furthermore, we show experimentally that the beamlike type-II SPDC offers the best biphoton single-mode coupling efficiency.

Let us first briefly discuss the emission properties of the three phase matching conditions of type-II SPDC for the conditions of our experiment. The pump laser was a 408 nm cw diode laser (Coherent Cube) and the SPDC photons had the central wavelength of 816 nm. A 2-mm- or a 4 mm-thick $\beta-\mathrm{BaB_2O_4}$ (BBO) crystal was used as the SPDC medium. For the collinear type-II SPDC, in which the pump laser and the SPDC photon pair propagates together, the optic axis angle (with respect to the pump laser) is calculated to be 41.5°. The tuning curve and the transverse emission pattern of the collinear type-II SPDC calculated for a 2-mm-thick BBO crystal is shown in Fig. 1(a). Here, we have assumed that the optic axis of the crystal lies in the vertical plane and the horizontal ($\theta_\parallel$) and the vertical ($\theta_\perp$) angles are measured from the pump beam. The 816 nm entangled photon pair propagates collinearly with the pump beam at $(\theta_\parallel, \theta_\perp) = (0, 0)$.

Noncollinear type-II SPDC, in which the entangled photon pair propagates at different angles, can be achieved by increasing the optic axis angle slightly. In the experiment, by increasing the optic axis angle to 42.3°, we achieved noncollinear photon pair emission such that the angle between the photon pair emission with respect to the pump beam is $(\theta_\parallel, \theta_\perp) = (\pm 3.3°, 0)$. Figure 1(b) shows the calculated tuning curve and the transverse emission pattern of the noncollinear type-II SPDC, which is often used to prepare polarization entangled photon pairs [4,11–14].

Finally, 816 nm centered beamlike photon pair emission in type-II SPDC can be accomplished by reducing the optic axis angle to 40.6°. At this angle, the pair photons are no longer emitted into two rings and the entangled (but not in polarization) photon pair is emitted as two vertically (in the optic axis plane) separated beams [9,10]. In our experimental condition, the pair photons are emitted at $(\theta_\parallel, \theta_\perp) = (0, \pm 3.3°)$ as shown in Fig. 1(c). Note the photons
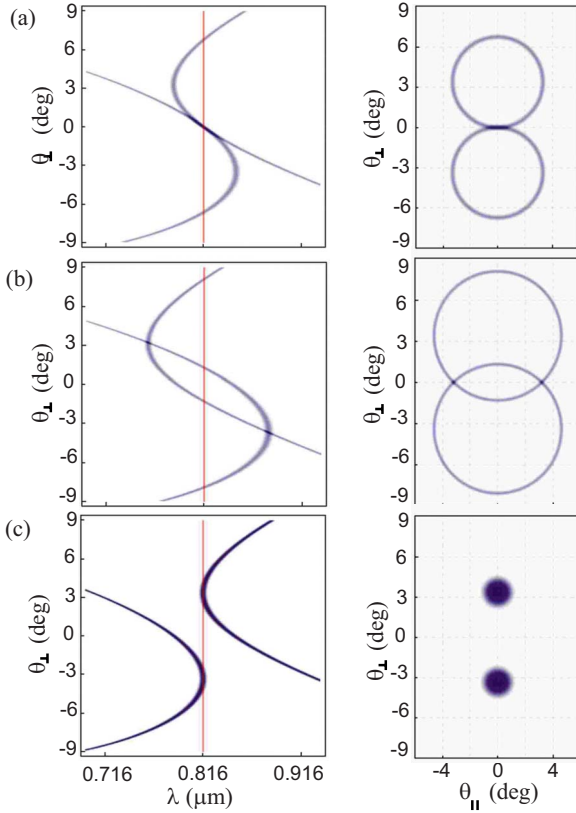
*yoonho@postech.ac.kr

FIG. 1. (Color online) Calculated tuning curves (left column) and transverse emission patterns (right column) of degenerate (816 nm) type-II SPDC from a 2-mm-thick BBO crystal. (a) collinear, (b) noncollinear, and (c) beamlike type-II SPDC.

are emitted in much broader ranges of angles in beamlike type-II SPDC. In addition, the tuning curve in Fig. 1(c) suggests that the emitted photons have spatially symmetric spectra in beamlike type-II SPDC.

To experimentally compare the biphoton single-mode coupling efficiencies for the three phase matching conditions of type-II SPDC, we set up the experiment as follows. The pump beam was focused at the BBO crystal using a lens with $f=300$ mm [11]. The pump power was measured to be 40 mW before the BBO. For the collinear case, the experimental schematic shown in Fig. 2(a) was used. The pump beam was removed by using a pair of pump-reflecting mirrors (PM) (antireflection coated for SPDC) and the orthogo-

nally polarized photon pair was separated spatially by using a polarizing beam splitter (PBS). An objective lens OL (Newport M-10X; 16.5 mm focal length, 7.5 mm clear aperture, and 0.25 numerical aperture) was used to couple the photon into a single-mode optical fiber (SMF) with the mode field diameter (at 850 nm) of roughly 5 μm and the numerical aperture of 0.13. The single-mode fiber has a cutoff wavelength of 730 ± 30 nm. The other end of the single-mode fibers are directly connected to single-photon detectors D1 and D2 (Perkin-Elmer SPCM-AQ4C). The coincidence events are measured with the 3 ns coincidence window. Interference filters (IFs) were placed in front of the objective lenses and Fig. 2(c) shows the measured transmission curves of the interference filters. (An Agilent 8453 UV/VIS spectrophotometer was used for this measurement.) For the noncollinear and beamlike cases, the experimental schematic shown in Fig. 2(b) was used and the BBO to OL distances are kept the same. Note that, for the beamlike case, the pump polarization and the BBO have to be rotated by 90° to keep the coupling optics in the same horizontal plane.

The SPDC single-mode coupling was achieved by initially placing the objective lens at 520 mm from the BBO so that the pump-mode (estimated to be 80 μm in diameter) at the BBO was mapped to the single-mode fiber core [11,14,19]. Further adjustments (transverse and longitudinal positions and tilt) were then made to the single-mode fiber, the objective lens, and the pump-focusing lens so as to maximize the coincidence count rate (R_c) as well as the single-detector count rates (R_1 and R_2). We then record the biphoton coupling efficiency defined as

$$\eta = R_c / \sqrt{R_1 R_2}.$$

The individual channel efficiencies η_1 and η_2 for D1 and D2, respectively, can be calculated by using the relation $\eta_1 = R_c / R_2$ and $\eta_2 = R_c / R_1$ [20]. Keep in mind that η, η_1, and η_2 are the overall efficiencies, i.e., they include losses due to interference filters, coupling optics, detector quantum efficiency, etc.

The experiment to measure the biphoton single-mode coupling efficiency were performed with a 2-mm-thick BBO and a 4-mm-thick BBO. In each case, two interference filter settings, 10 and 80 nm full width at half maximum (FWHM), were used to measure the single-mode coupling efficiency. The results of the single-mode coupling measure-
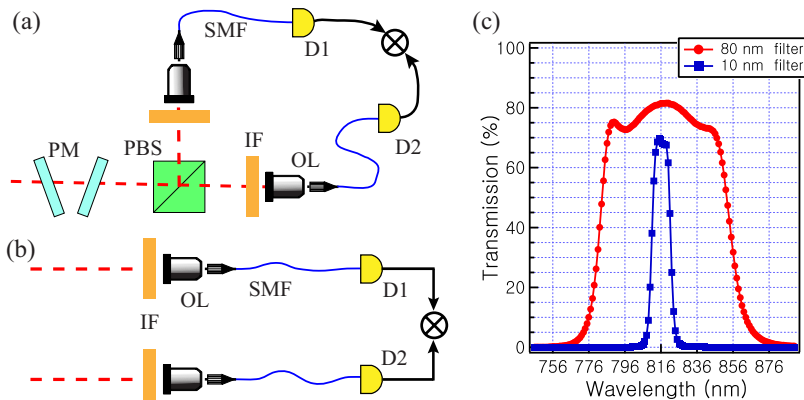

FIG. 2. (Color online) Schematic for testing biphoton single-mode coupling efficiencies for (a) collinear type-II SPDC and (b) noncollinear and beamlike type-II SPDC. (c) Measured transmission curves of the interference filters (IFs) used in this experiment.
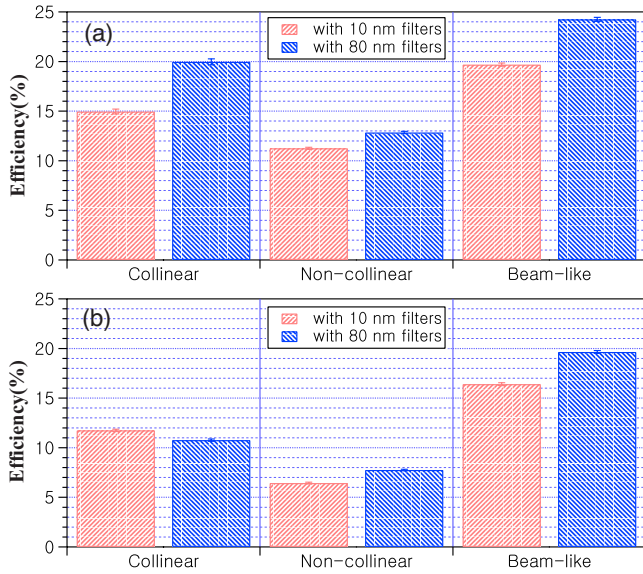
FIG. 3. (Color online) Type-II SPDC biphoton single-mode coupling efficiencies. (a) 2-mm-thick BBO. The maximum coincidence count rates were ~20 kHz for both the collinear and the noncollinear schemes and ~32 kHz for the beamlike scheme. (b) 4-mm-thick BBO. The maximum coincidence rates were ~15 kHz for both the collinear and noncollinear schemes and ~43 kHz for the beamlike scheme.

ments are reported in Fig. 3. In Fig. 3(a), we report the single-mode coupling efficiencies for a 2-mm thick BBO and in Fig. 3(b), for a 4-mm-thick BBO.

As theoretically discussed in Refs. [14,19], the experimental data in Fig. 3 shows the fact that a thinner crystal offers better biphoton single-mode coupling efficiencies than a thick one. The data also provide a few interesting new experimental findings. First, as analyzed in Ref. [19], the collinear case offers better biphoton single-mode coupling than the noncollinear case. Second, the beamlike condition offers the best biphoton single-mode coupling in type-II SPDC, even though the actual transverse spatial distribution is broader than those of the collinear and the noncollinear cases, as shown in Fig. 1.

In our experiment, the highest biphoton single-mode coupling efficiency achieved was $\eta = R_c/\sqrt{R_1 R_2} = 24.2\%$ for the beamlike case, Fig. 3(a). Since η is the overall efficiency which includes the losses in the optical path, it is important to identify known sources of losses in the experimental setup and they include the interference filters, the single-photon detectors, and the single-mode fibers [21]. First, the loss due to the interference filters were accurately characterized by using a spectrophotometer and the results are shown in Fig. 2(c). Second, the loss at the single-photon detector is due to less than unity detection efficiencies of the detectors and the quantum efficiency of the detectors is found to be roughly 50% on average across the wavelength region of interest [22]. Finally, the process of coupling SPDC photons into the single-mode optical fiber inevitably introduces a large loss. We used a He-Ne laser to measure the single-mode coupling efficiency to be 61%. This number, however, should be taken as a rough estimate only as there are uncertainties due to the

fact that (i) the actual working wavelength is 816 nm while the efficiency measurement was done at 633 nm and (ii) unlike the He-Ne laser, the spatial profiles of the 408 nm diode pump laser and the SPDC are not Gaussian shaped.

Recent studies assume a suitably focused Gaussian-shaped pump laser beam at the BBO crystal when calculating the optimal single-mode coupling conditions of SPDC [11,12,17–19], but the diode laser used in our work provided strongly elliptical spatial mode profile. As a result, the biphoton single-mode coupling efficiencies achieved in this experiment are consistently lower than the theoretically calculated values (after factoring-in known losses) reported in Refs. [14,19] and experimental results reported in a few recent works using the noncollinear scheme [11–13]. We, however, note that the aim of this work is to directly compare single-mode coupling efficiencies of three phase matching conditions of type-II SPDC in the same experimental conditions, and we expect to observe significant improvement of the biphoton coupling efficiencies if the pump mode can be properly shaped into a Gaussian profile [11–14].

Another important factor which affects the biphoton coupling efficiency η heavily is the quality of conjugate mode selection. In the case of single-mode coupling, since we are mapping the pump mode at the BBO to the cores of the single-mode fibers by using objective lenses with large clear aperture, the problem of conjugate mode selection is related to the mismatch of the numerical apertures of the objective lens and the single-mode fiber. For the data shown in Fig. 3, the numerical apertures of the objective lens ($\times 10$) and the single-mode fiber are, respectively, 0.25 and 0.13. In Fig. 4, we show the efficiency measurement data for a 4-mm-thick type-II BBO using the $\times 20$ objective lens (Newport M-20X; 9.0 mm focal length, 6.0 mm clear aperture, and 0.40 numerical aperture). Clearly, increased mismatch of the numerical apertures causes degradation of the biphoton single-mode coupling efficiencies in all phase matching conditions of type-II SPDC.

It is therefore reasonable to assume that further improvement of the biphoton single-mode coupling efficiency is possible by reducing the numerical aperture of the objective lens to match that of the single-mode fiber. However, this will make the overall system size (BBO to the objective lens) bigger, which could be less desirable in some cases. In addition, to match the dimension of the pump laser at the BBO and the size of the core of the single-mode fiber, it will require tighter focusing of the pump at the crystal. Tighter focusing, however, is only reasonable if the pump laser is Gaussian-shaped. Furthermore, it is known to cause undesirable spectral broadening and asymmetry in type-II SPDC which in turn have the effect of reducing quantum correlations in the polarization degrees of freedom [23]. Thus, optimization of the biphoton single-mode coupling efficiency in type-II SPDC will require compromises based on which physical effects are to be utilized in experiments.

In addition, it is not immediately clear whether the reduced efficiency of the single-mode coupling due to a non-Gaussian shaped focused pump beam contributes equally to the three type-II phase matching conditions. Since the transverse mode profiles of SPDC are quite different for different phase matching conditions, see Fig. 1, and the SPDC from
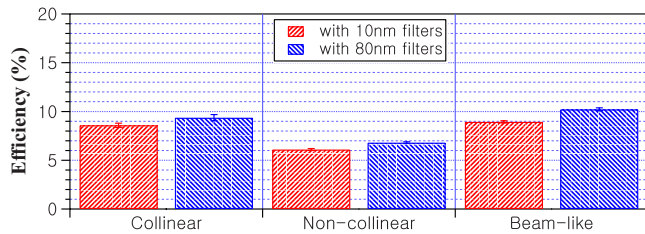
FIG. 4. (Color online) Type-II SPDC biphoton single-mode coupling efficiencies. The data are for a 4-mm-thick type-II BBO crystal using $\times 20$ objective lenses. The maximum coincidence rates were $\sim$7.7 kHz for both the collinear and noncollinear schemes and $\sim$11 kHz for the beamlike scheme.

focused pump shows asymmetrical transverse distribution patterns [24], it is possible that the single-mode coupling efficiencies of the three phase matching conditions are affected differently by the non-Gaussian shaped pump. Further theoretical studies would be needed to accurately quantify such an effect.

In summary, we have experimentally investigated the biphoton single-mode coupling efficiencies of the collinear, noncollinear, and beamlike type-II SPDC under the same experimental conditions. We have found that, in agreement with the theoretical predictions in Ref. [19], the collinear case showed better coupling efficiency than that of the noncollinear case. In addition, we have shown experimentally that the beamlike case, among the three phase matching regimes of type-II SPDC, indeed offers the best biphoton single-mode coupling efficiency, although its transverse spatial distribution is broader than those of the collinear and noncollinear cases.

[1] D. N. Klyshko, *Photons and Nonlinear Optics* (Gordon & Breach, New York, 1988).
[2] Y. H. Shih and C. O. Alley, Phys. Rev. Lett. **61**, 2921 (1988).
[3] C. K. Hong, Z. Y. Ou, and L. Mandel, Phys. Rev. Lett. **59**, 2044 (1987).
[4] P. G. Kwiat, K. Mattle, H. Weinfurter, A. Zeilinger, A. V. Sergienko, and Y. Shih, Phys. Rev. Lett. **75**, 4337 (1995).
[5] Y.-H. Kim and W. P. Grice, Opt. Lett. **30**, 908 (2005).
[6] S.-Y. Baek and Y.-H. Kim, Phys. Rev. A **77**, 043807 (2008).
[7] T. E. Kiess Y. H. Shih, A. V. Sergienko, and C. O. Alley, Phys. Rev. Lett. **71**, 3893 (1993).
[8] T. B. Pittman Y. H. Shih, A. V. Sergienko, and M. H. Rubin, Phys. Rev. A **51**, 3495 (1995).
[9] S. Takeuchi, Opt. Lett. **26**, 843 (2001).
[10] Y.-H. Kim, Phys. Rev. A **68**, 013804 (2003).
[11] C. Kurtsiefer, M. Oberparleiter, and H. Weinfurter, Phys. Rev. A **64**, 023802 (2001).
[12] J. Volz, C. Kurtsiefer, and H. Weinfurter, Appl. Phys. Lett. **79**, 869 (2001).
[13] C. Kurtsiefer, M. Oberparleiter, and H. Weinfurter, J. Mod.

Opt. **48**, 1997 (2001).
[14] F. A. Bovino *et al.*, Opt. Commun. **227**, 343 (2003).
[15] M. Fiorentino, C. E. Kuklewicz, and F. N. C. Wong, Opt. Express **13**, 127 (2005).
[16] A. Fedrizzi *et al.*, Opt. Express **15**, 15377 (2007).
[17] A. Dragan, Phys. Rev. A **70**, 053814 (2004).
[18] R. Andrews, E. R. Pike, and S. Sarkar, Opt. Express **12**, 3264 (2004).
[19] S. Castelletto *et al.*, New J. Phys. **6**, 87 (2004).
[20] D. N. Klyshko, Sov. J. Quantum Electron. **10**, 1112 (1980).
[21] There are Fresnel reflection losses due to BBO surfaces, detector windows, and miscellaneous optical components that we have not quantitatively accounted for but we expect this to be less than 10% per optical channel.
[22] http://www.perkinelmer.com/opto
[23] Z. Zhao, K. A. Meyer, W. P. Whitten, R. W. Shaw, R. S. Bennink, and W. P. Grice, Phys. Rev. A **77**, 063828 (2008).
[24] R. S. Bennink, Y. Liu, D. D. Earl, and W. P. Grice, Phys. Rev. A **74**, 023802 (2006).